DISCLAIMER FOR FRONT PAGE OF MATERIALS TO BE MADE AVAILABLE VIA ETI INTERNET SITE

1. "Save to the extent set out in paragraph 2 below, this document and its contents are made available to you via the ETI's Internet Site "as is" without any representations, conditions, warranties or other assurance of any kind. The ETI and the authors, together with their employees, directors, servants or agents exclude to the maximum extent permissible by law all representations, warranties, conditions or other assurance whatsoever (whether express or implied) regarding the use of this document or its content including any warranties of title, merchantability, accuracy, completeness, non-infringement or that the document or its contents are of satisfactory or any particular quality or fit for any particular purpose. Any person accessing this document and using it or any of its contents accepts all risk in doing so.
2. Notwithstanding any statement to the contrary contained on the face of this document, the ETI confirms that the authors of the document have consented to its publication by the ETI."

ReDAPT MC7.1

Initial Operation Power Curve

DOCUMENT CONTROL

I						
H						
G						
F						
E						
D						
C						
B						
A	06/05/2014	J. MCNAUGHTON	R. SINCLAIR S. HARPER	D. DOBSON	Updated for new deployment data.	GFE
-	31/07/2013	S. HARPER	R. SINCLAIR	P. CHESMAN		GFE
Rev	Date	Established	Checked	Approved	Modifications	Status (*)

(*) PREL : Preliminary, GFA : Good for Approval, GFE: Good for Execution

DOCUMENT EVOLUTION

Rev	DATE	CHAPTER	PAGE	MODIFICATION
-	31/07/2013	All	All	First issue
	06/05/2014	All	All	Rewrite for new deployment data, IEC 62600-200:2013(E) format

DOCUMENT DISTRIBUTION

TO BE DISTRIBUTED TO (FUNCTION)	NAME
ETI	S. Swatton
ReDAPT Programme Manager	D. Dobson
Engineering Director	J. Rhymes
Performance Engineer	B. Kerling, J. Bossard, S. Harper
Electrical Engineering Manager	P. Le Quéau
Development Engineering Manager	J. Bishop
Design Engineering Manager	F. Pilorge
Commercial Manager	A. Alliston
Controls Engineering Manager	A. Colin

TABLE OF CONTENTS

1 REFERENCES

Bahaj, A. S., Batten, W. M., & McCann, G. (2007). Experimental verifications of numerical predictions for the hydrodynamic performance of horizontal axis marine current turbines. *Renewable Energy, 32*.

Drela, M. (n.d.). *Xfoil*. Retrieved April 10, 2014, from http://web.mit.edu/drela/Public/web/xfoil/

Garrett, C., & Cummins, P. (2007). The efficiency of a turbine in a tidal channel. *Journal of Fluid Mechanics, 588*.

Grasso, F. (2010). Usage of Numerical Optimization in Wind Turbine Airfoil Design. *28th AIAA Applied Aerodynamics Conference*. Chicago.

IEC. (2013). *Marine Energy - Wave, tidal and other water energy converters - Part 200: Electricity producing tidal energy converters - Power performance assessment.*

Newton, P. (2012). *DEEPGen IV 1MW Tidal Turbine Loads - Certification Report for GL Design Assesment.*

Nishino, T., & Willden, R. (2012). The efficiency of an array of tidal turbines partially blocking a wide channel. *Journal of Fluid Mechanics, 708*.

Palethorpe, B. (2013). *Calculating turbine power output from on-shore power measurements on Eday.*

Smith, S. (2014). *MA1001 ReDAPT MD6.2 - Environment Modelling Validation Report.* ETI.

van Rooij, R. (1996). *Modification of the boundary layer calculation in RFOIL for improved airfoil stall prediction.*

Way, S., & Thomson, M. (2011). *MA1001 ReDAPT MD6.1 - Site Characterisation and Design Basis Report.* ETI.

Whelan, J. I., Graham, J. M., & Peiró, J. (2009). A free-surface and blockage correction for tidal turbines. *Journal of Fluid Mechanics, 624*.

Note: these reports have been submitted and approved by the ETI as part of the ReDAPT project but are not in the public domain. Their inclusion in the list of references is to aid transparency in the production of this document.

** Note: these reports are internal to Alstom Ocean Energy and are not in the public domain. Their inclusion in the list of references is to aid transparency in the production of this document.

2 ACROYNMS

ADCP	Acoustic Doppler Current Profiler
BEMT	Blade Element Momentum Theory
BNG	British National Grid
DG	DEEP-Gen
HAT	Highest astronomical tide
LAT	Lowest astronomical tide
LSS	Low-Speed Shaft
MSL	Mean Sea Level
NW	North West
QC	Quality Control
ReDAPT	Reliable Data Acquisition Platform for Tidal
RMS	Root Mean Square
SE	South East
TEC	Tidal Energy Converter
UT	Universal Time
VSPR	Variable Speed Pitch Regulated
WGS	World Geodetic System

3 INTRODUCTION

This document presents the power curve calculated for DEEP-Gen IV, a horizontal axis tidal energy converter (TEC). The test procedure is conducted as part of the Reliable Data Acquisition Platform for Tidal (ReDAPT) project during the TEC's deployment in the fourth quarter of 2013 at the European Marine Energy Centre (EMEC) at the Fall of Warness.

DEEP-Gen IV is a commercial scale turbine not designed for production. Rather, it is used to prove the concept and technology whilst acting as a development stage for the next generation of Alstom Ocean Energy turbines. This document is intended to show the measured power curve and validate the predicted power curve produced using Tidal Bladed. This software can then be used to produce power curves for the next generation of turbines.

This document has been produced in line with the recommendations laid out in the IEC 62600-200 Standards (IEC, 2013).

4 TEC REPORT

4.1 TEC description

The TEC is a three blade horizontal-axis tidal turbine with Variable Speed Pitch Regulated (VSPR) control. The turbine yaws in each slack tide so that its energy extraction plane is perpendicular to the principal flow direction and upstream of the turbine nacelle. The turbine parameters are shown in Table 4-1 with an overview of the design in Figure 4-1.

Make	Alstom
Type	Three blade horizontal axis tidal turbine
Serial number	DG4
Production year	2011
Blade radius	9.04m
Equivalent diameter	18.08m
Projected capture area	256.74m^2
Distance above sea bed	19m (turbine centreline)
Foundation	Piled tripod

Table 4-1: Key parameters of the TEC

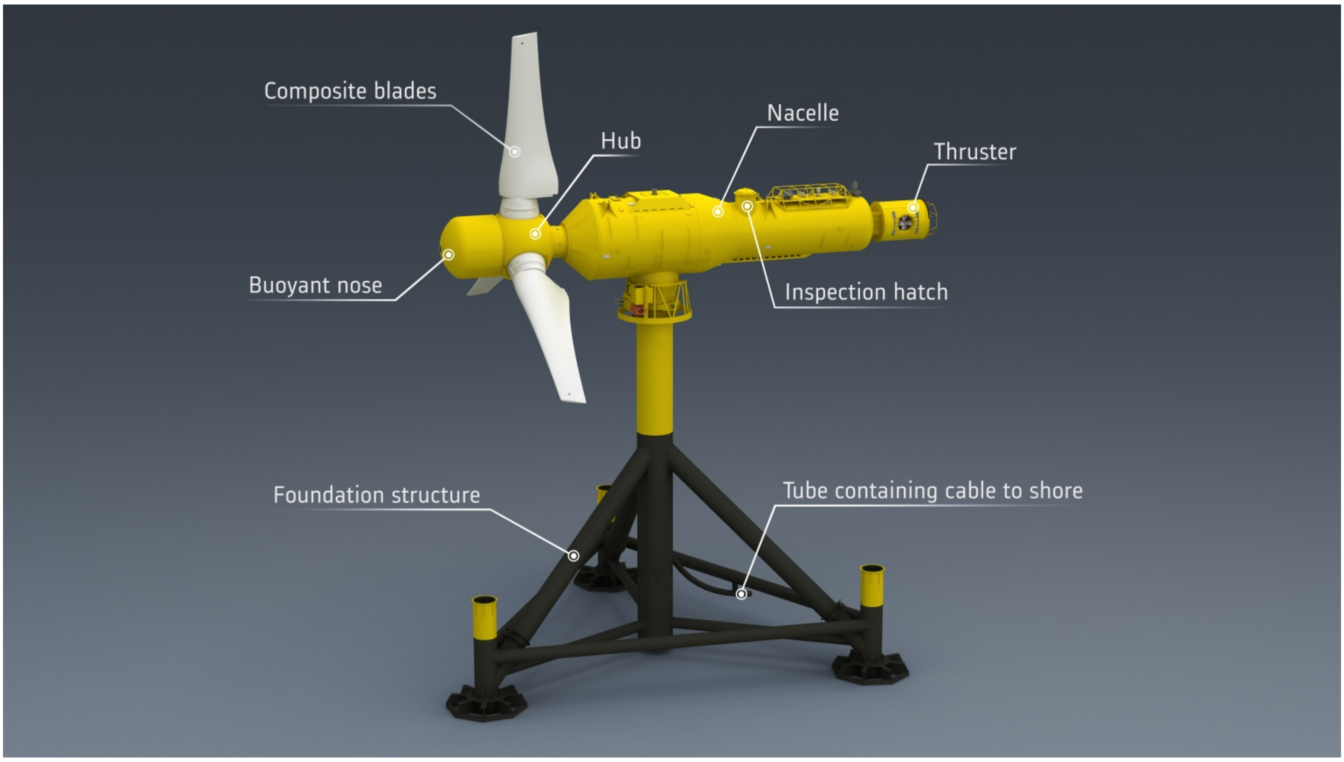

Figure 4-1: Overview of the TEC.

4.2 Power take-off

The power take-off system is defined by the parameters in Table 4-2 and described by the image and diagram in Figure 4-2.

Generator rated voltage	690 V
Generator current	1165 A
Generator frequency rating (Grid side)	50 Hz
Converter rated voltage	650 V
Converter current (Grid side)	1100 A
Converter frequency rating	50 Hz

Table 4-2: Power take-off system parameters

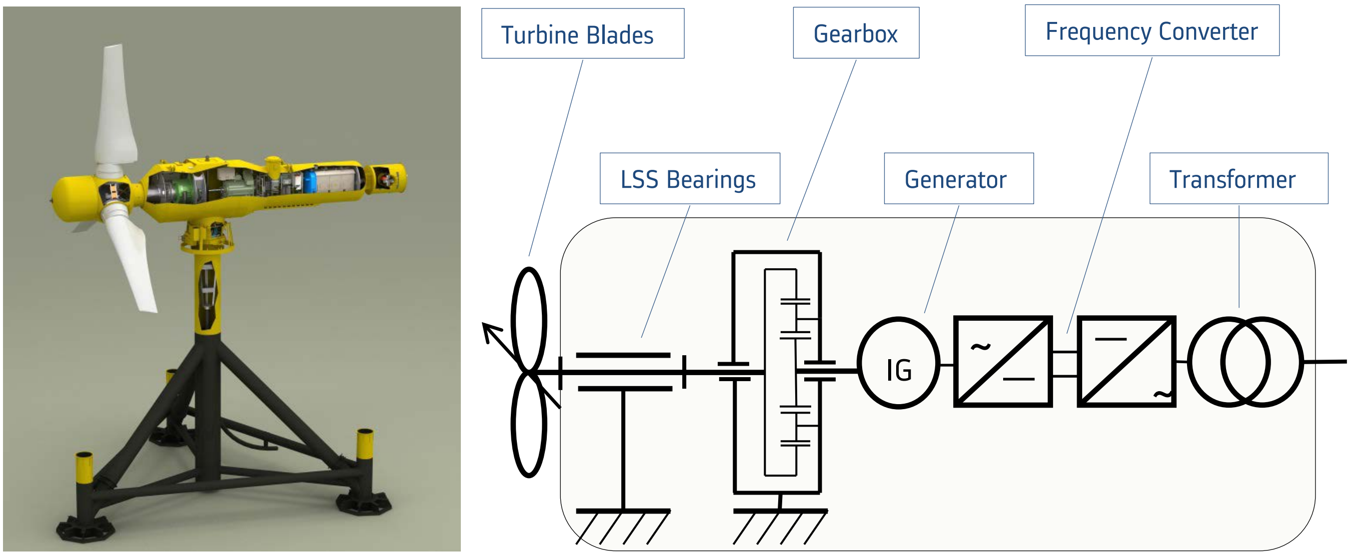

Figure 4-2: Overview of power take-off system

4.3 Operational Parameters

The turbine is designed to cut-in at a velocity at the start of the tidal cycle up to a rated velocity where the rated output power is produced. The key parameters are defined in Table 4-3.

Rated output power	1.0 MW
Rated water velocity	2.7 m/s
Diameter	18.08 m
Overhang (rotor to tower distance)	0.7 m
Cut-in water velocity	1.0 m/s
Nominal rotor speed	13.78 rpm
Maximum rotational speed	19.29 rpm

Table 4-3: Key turbine operational parameters

5 TEC TEST SITE REPORT

5.1 Site Description

The TEC is placed in the Fall of Warness at the EMEC test site. The location of the TEC is shown in Table 5-1. A description of the bathymetric features is shown in Figure 5-1.

TEC location	EMEC test site, Fall of Warness
Location (WGS84 coordinate system)	59.136853N, 2.805833W
Location (BNG coordinate system)	1028061N, 353986E
Electrical cable length to shore	3.6k m

Table 5-1: Description of test side for obtaining power curve data

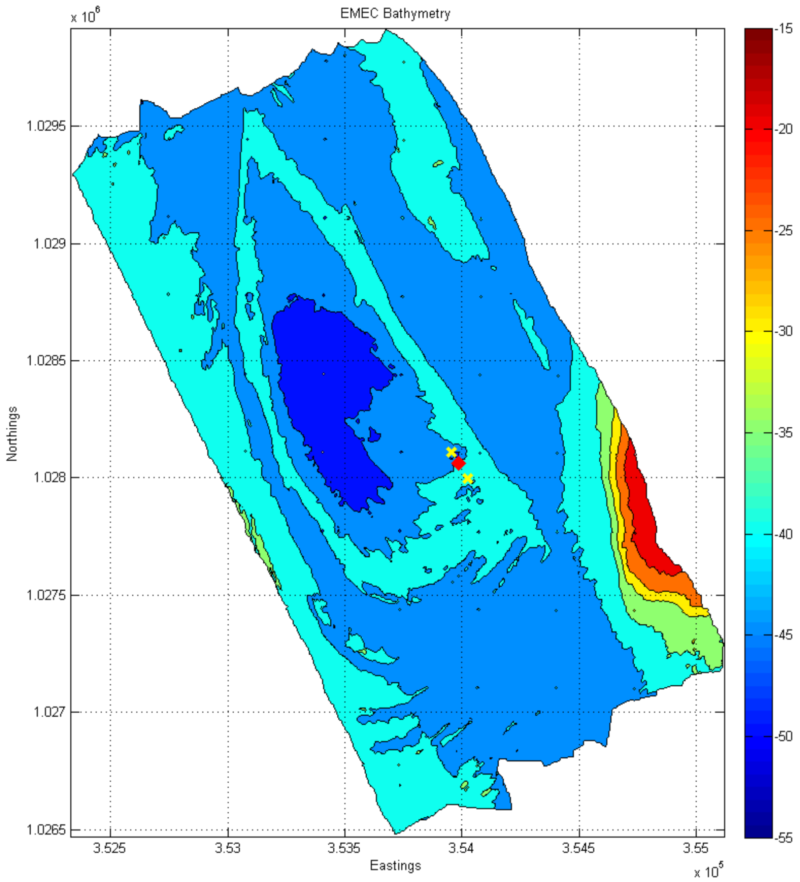

Figure 5-1: Bathymetry (depth below MSL in m), TEC shown as red diamond and ADCPs as yellow crosses. Map uses BNG coordinate system and note difference in x and y axis scales.

Mean Sea Level (MSL) relative to chart datum	1.51 m
Highest astronomical tide (HAT) relative to chart datum	2.97 m
Lowest astronomical tide (LAT) and chart datum from seabed	41.57 m
Long term mean current	1.804 m/s
Long term mean flood current	1.701 m/s

Long term mean ebb current	1.896 m/s
Mean spring peak current	3.079 m/s
Mean neap peak current	1.744 m/s
Principal flood direction (from North)	137°
Principal ebb direction (from North)	331°

Table 5-2: Environmental conditions at the EMEC test site taken from ReDAPT report MD6.1 (Way & Thomson, 2011)

5.2 Environment conditions

Environmental conditions that define the EMEC test site were measured as part of the ReDAPT project and listed in report MD6.1 (Way & Thomson, 2011); key parameters for the power curve creation are listed in Table 5-2. A tidal ellipse of data used for the power curve creation in this report is shown in Figure 5-2. Note that the bin data is ten-minute power-weighted velocities over the rotor area (see Section 9.2) and does not agree with the principal flow directions from MD6.1 (Way & Thomson, 2011) which have been derived using depth-averaged velocity. Analysis of depth profiles at the EMEC site were conducted in MD6.2 (Smith, 2014) and showed the directional twist changed significantly through the water column by as much at 10° from the mean. This would contribute towards the differences in principal and bin-data flow directions observed here. The reason for the different method of calculating flow velocity and direction is that the present report follows the method required by the IEC Standards (IEC, 2013) and described in Section 9.2.

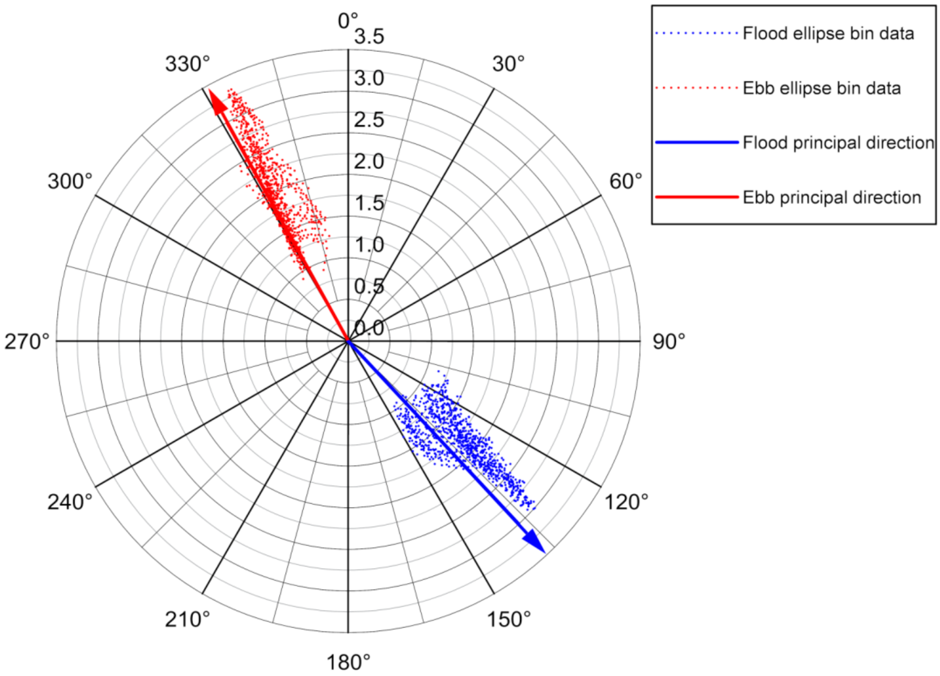

Figure 5-2: Tidal ellipse of flood and ebb bin data used for power curve creation

5.3 ADCP locations

The velocity used to characterise the power curve is obtained by means of two Acoustic Doppler Current Profilers (ADCPs) positioned to the North West (ADCP NW) and South East (ADCP SE) of the TEC location. The locations are shown in Table 5-3 with their location relative to the TEC in Figure 5-3. For analysis of data in a flood tide ADCP NW is used to characterise the flow, and for an ebb tide ADCP SE is used. Figure 5-3 shows the offset of the ADCP from the relevant principal flow directions is 1.5D for ADCP NW and 0.2D for ADCP SE and that they are positioned 3.38D and 4.26D upstream of the TEC foundation centre when defining the flow velocity. Section 8.9.1A of the IEC Standards (IEC, 2013) shows that for inline capture, the ADCPs meet all of the criteria except for ADCP SE's offset from the principal ebb flow direction which should be within ±0.5D of the centre line. Direction measurements at both ADCP locations and turbine have been shown to be consistent in terms of both velocity magnitude (Smith, 2014) and direction and so it is hypothesised that the offset of ADCP SE does not have a significant impact on results. Note that 1D is 18.08 m and the plane of the rotor is 0.7D upstream of the TEC foundation centre.

From this analysis improved locations for the position of the ADCPs in future deployments were advised.

TEC	59.136853N, 2.805833W
ADCP NW	59.137284N, 2.806425W
ADCP SE	59.136492N, 2.805067W

Table 5-3: Locations of ADCPs used for velocity data capture

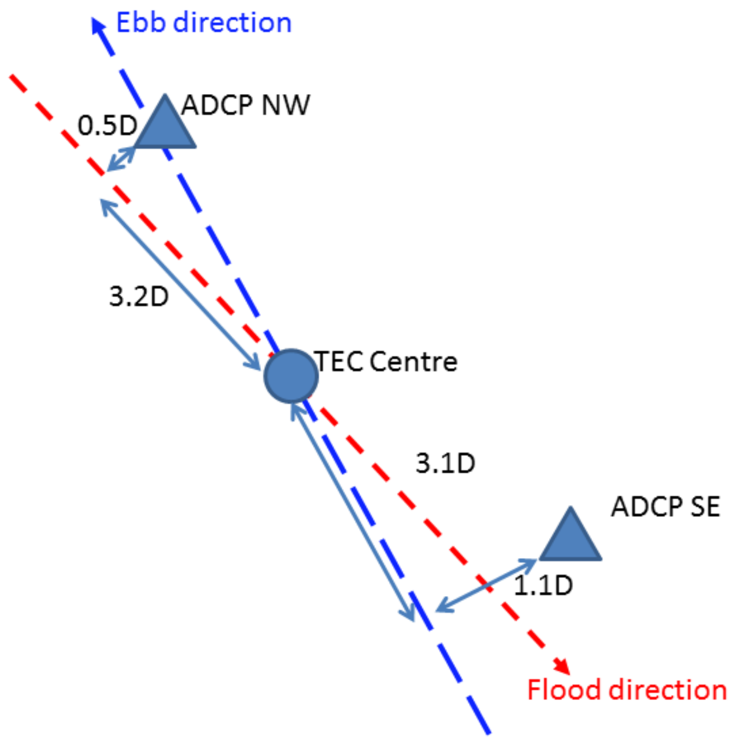

Figure 5-3: Layout of ADCPs compared to TEC and principal Flood and Ebb flow directions

6 ELECTRICAL GRID AND LOAD REPORT

Grid parameters are listed in Table 4-2.

7 TEST EQUIPMENT REPORT

The three velocity components are recorded using ADCP NW and ADCP SE, both devices are of equal specification as described in Table 7-1.

Instrument	600 kHz ADCP
Sampling frequency (Hz)	0.5
Sensor height above bed (m)	0.6
Bin size (m)	1.0
First bin centre (m)	2.07

Table 7-1: Specification of ADCPs used in velocity data acquisition

8 MEASUREMENT PROCEDURE REPORT

This report uses the Universal Time (UT) time zone, equivalent to GMT. Where data sets were obtained in other time references these were corrected prior to analysis.

The coordinate system used throughout this report is the World Geodetic System (WGS) 84 with values presented in decimal format of longitude and latitude. In one case it is necessary to display a chart (Figure 5-1) using the British National Grid (BNG) coordinate system.

No offset to account for drift between the ADCPs and the TEC is applied. Given the distance between the ADCPs and the TEC and the rate of velocity acceleration / deceleration any correction would be of the order of seconds and is deemed negligible when considering the sample period of 600 seconds.

The ADCP data is recorded at a frequency of 0.5Hz. The data processing procedure is as follows:

1) Data is recorded as raw "beam" data values;
2) Dropped data values are replaced with null values;
3) If the null values have no neighbours they are linearly interpolated;
4) Data is converted into instrument x, y, z coordinate system, taking into account co-sampled pitch and roll;
5) Heading data is applied to convert coordinates into East, North and Up;
6) E,N,U data is passed through 2 filters:
    a. Rejection of velocities not having a Minimum Amplitude of Signal Return;
    b. Outlier rejection based on windowed standard deviation;
    c. Phase-space iterative filtering can be applied to but was not used here.

Both filtering thresholds (minimum amplitude and multiplier/gain of the running-standard-deviation of the signal method) were set low in the data sets supplied for the creation of this power curve. For minimum amplitude this is unlikely to have rejected any data points. However, this has a small impact (1%) in the value of the mean velocity obtained after ensemble averaging over the (approximate) 300 data points making up a ten minute sample.

The low setting of the second filter (6b above) means only large outliers would be rejected; again this is unlikely to impact on the analysis due to the methodology it is used for here. For higher sensitivity analysis, such as analysis of turbulence, a tighter threshold would be required.

The 0.5Hz ADCP data was averaged into five minute samples before the method of bins was applied which resamples the data in to ten-minute samples. The turbine power was recorded at a frequency of 10Hz which is then filtered into 1Hz data using a low-pass filter with a time constant of 3 seconds.

9 PRESENTATION OF MEASURED DATA

9.1 Overview

This section details the data that is used for the power curve creation in the next section. Section 8.3 of the IEC Guidelines (IEC, 2013) specify that data should be collected over a minimum of 15 days to ensure a spring-neap cycle is observed, with the maximum duration allowed being 90 days. Availability over the test period should exceed 80%.

For the current power curve a 19 day sample is used, described in Table 9-1. Data was split into a flood or ebb data set based on the direction of the flow. The direction was evaluated by fitting a Bessel function to the raw direction data to improve the signal quality. Flood data was chosen if the direction of ADCP NW was positive and ebb data if the direction of ADCP SE was negative. The calculated time at either flood or ebb time is shown in the first row of Table 9-2.

Data is only presented on the power curve when the minimum power is greater than zero; this represents 42% of the 19 day sample. When considered with the slack tide the test availability is 72%. The remaining 28% of excluded data is accounted for by three main categories:

1. Tests conducted as part of the ReDAPT project to better understand flow data;
2. Tests conducted on the TEC operation;
3. Shutdowns of the TEC due to the controller due to, for example, flow conditions outside of the operating envelope.

These are all valid exclusions under section 8.5, data processing, of the IEC Standards (IEC, 2013). Future TEC deployments give the opportunity to increase the data availability and to reach the 80% availability specified by the IEC Standards (IEC, 2013).

Start of sample	15/10/2013 14:00
End of sample	3/11/2013 14:00

Table 9-1: Dates of data collection for power curve creation

	Flood	Ebb	Total
Tide by ADCP direction	48%	50%	98%
Time at slack ($U<1ms^{-1}$)	15%	15%	30%
Minimum Power > 0	22%	20%	42%
Minimum Power > 0 + Slack	37%	35%	72%

Table 9-2: Overview of sampled data used for power curve creation, shown as a percentage of the 19 day sample

9.2 Method of bins

Data is sampled into ten-minute bins and presented against mean power-weighted tidal-current velocity. This procedure follows the method of bins as laid out in the IEC Standards (IEC, 2013) and described here. The integral of the cube of the velocity upstream of the TEC over the turbine area is calculated and then averaged over the chosen sampling period, here 10 minutes.

This integral, or power weighted tidal current velocity, $\underline{\widehat{U}_t}$, is calculated as:

$$\underline{\widehat{U}_j} = \left[\frac{1}{A}\sum_{k=1}^{S} \underline{U}_{k,j}^{3} A_k\right]^{1/3},$$

Where:

$$A = \sum_{k=1}^{S} A_k,$$

And: j is the index of the time instant, k is the index of the ADCP bin, S is the number of ADCP bins over the turbine area, A is the projected capture area of the TEC [m^2], A_k is the projected capture area of the TEC corresponding to ADCP bin k [m^2], $\underline{U}_{k,j}$ is the velocity vector at time index j and ADCP bin index k [ms^{-1}]. See Figure 9-1 for definition of these.

$\underline{\widehat{U}}_j$ is then averaged into bins corresponding to the required sampling period, which here is ten minutes. It is also important to note that the velocity data used in this analysis had already been averaged into step sizes of 5 minutes.

There is a difference in depth between the ADCP locations and a 2° tilt of the turbine nacelle from the horizontal between flood and ebb positions. Due to these the selected bins and their weighting coefficients used in the method of bins are different for each ADCP; this is explained by Figure 9-2. The 2° tilt of the rotor was not factored into any of the equations, i.e. the "effective rotor area" was not reduced.

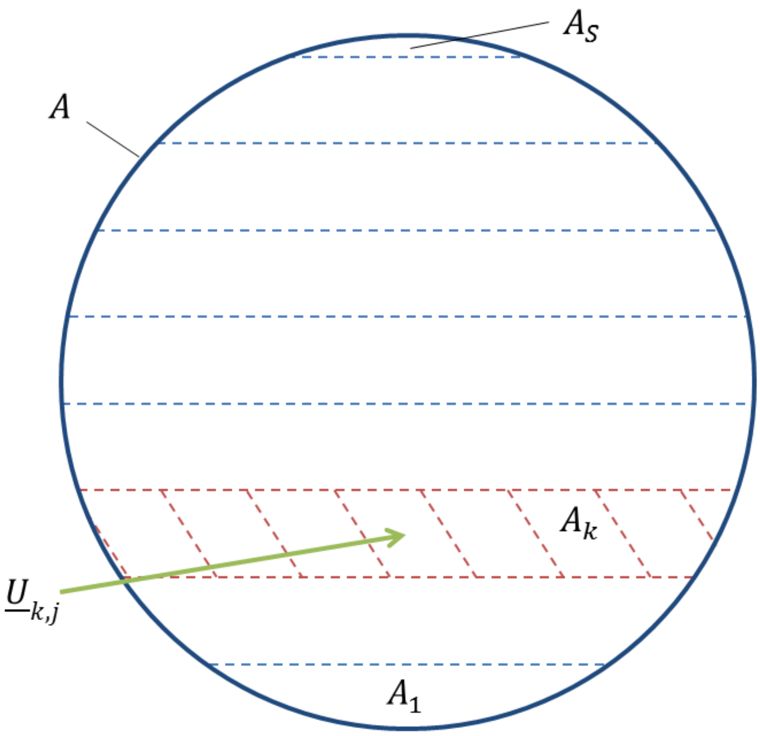

Figure 9-1: Rotor areas definition for method of bins

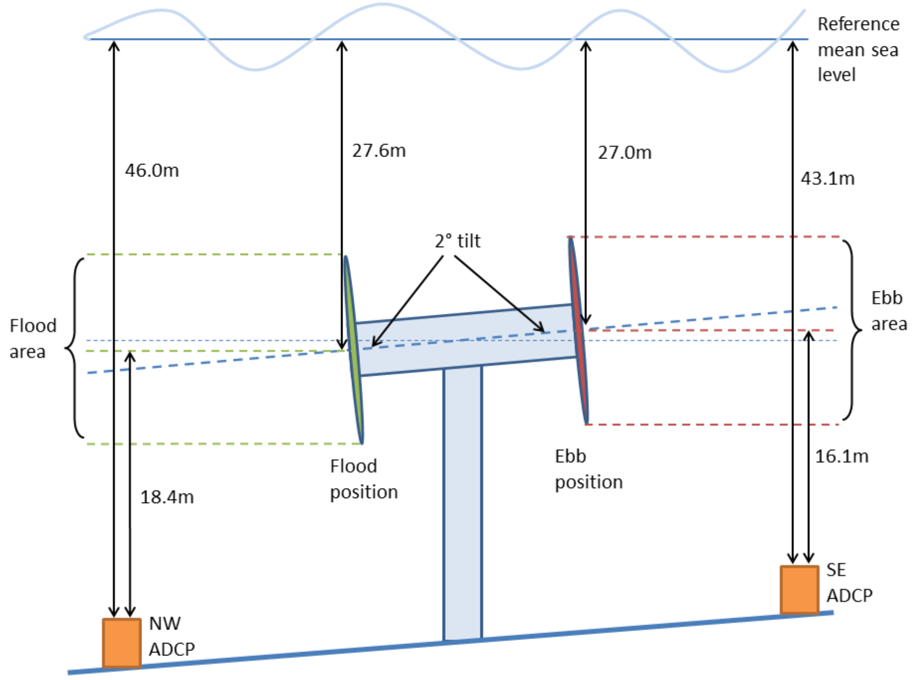

Figure 9-2: Plot of TEC to give flood and ebb areas used in method of bins. Not to scale.

9.3 Data Inclusion and Exclusion

Data is presented that met the criteria that the turbine was generating and not non-operational due to slack tides. In addition, due to specific tests being carried out as part of the ReDAPT program, further data was excluded from the data sets. This latter set of excluded data is shown in Figure 9-3 for both flood and ebb tides.

9.4 Power Curve Data

Data used for the creation of the power curves is shown in Figure 9-4 and Figure 9-5 for the flood and ebb tides respectively. For each of the ten-minute samples the maximum, mean, minimum and standard deviation of the power is presented. The data is plotted against the corresponding ten-minute power-weighted current velocities. More scatter in the data is observed for the ebb tide which is partially due to data being collected over a larger range of velocities. A greater standard deviation was witnessed on the flood tide, which confirms previous studies that identified flood as being the more turbulent tide (2) (3).

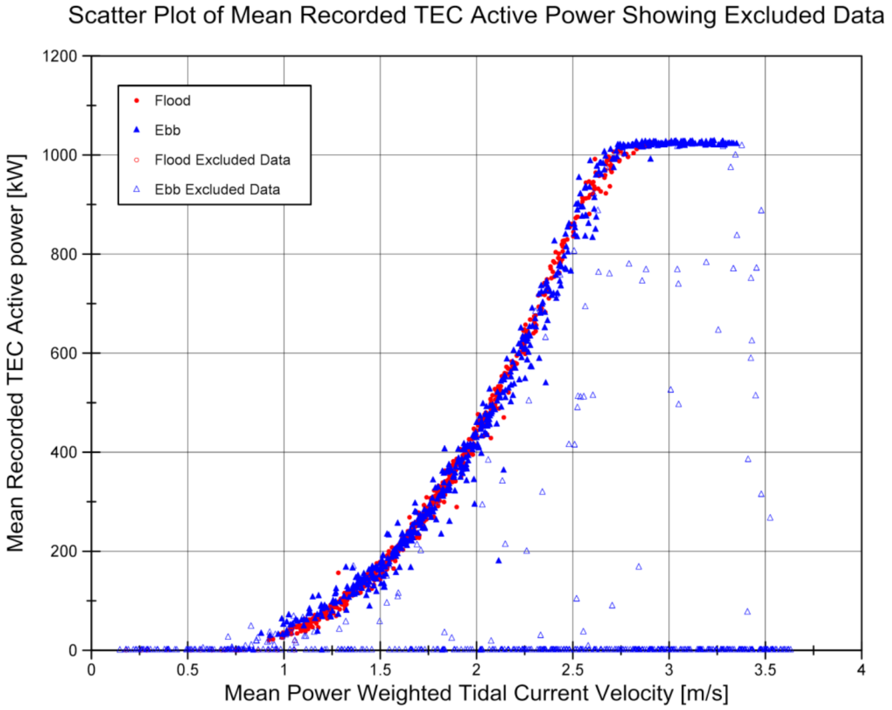

Figure 9-3: Plot showing data excluded from flood and ebb measurements

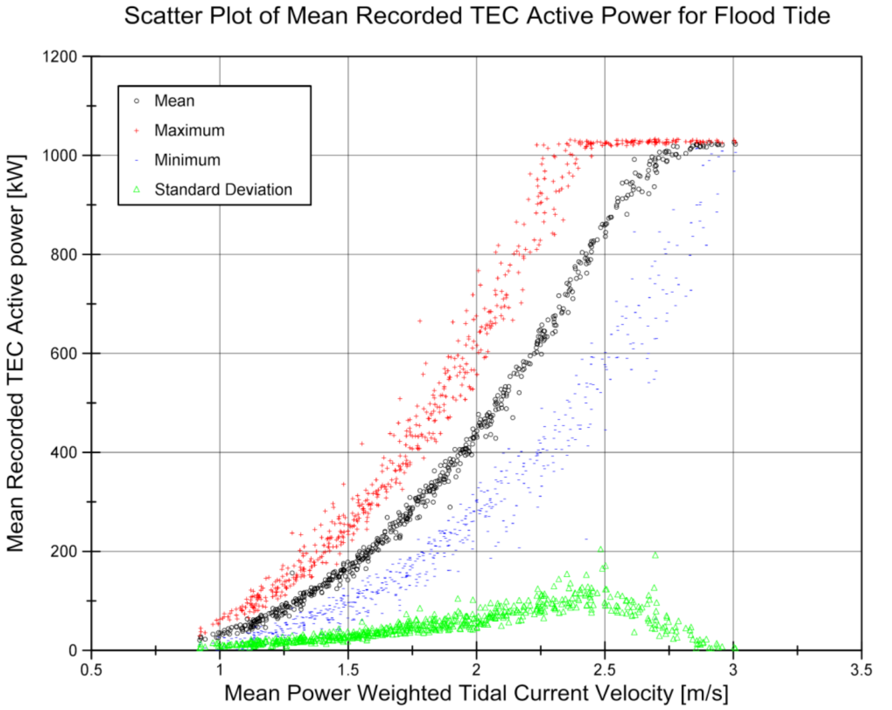

Figure 9-4: Active recorded power for flood tide

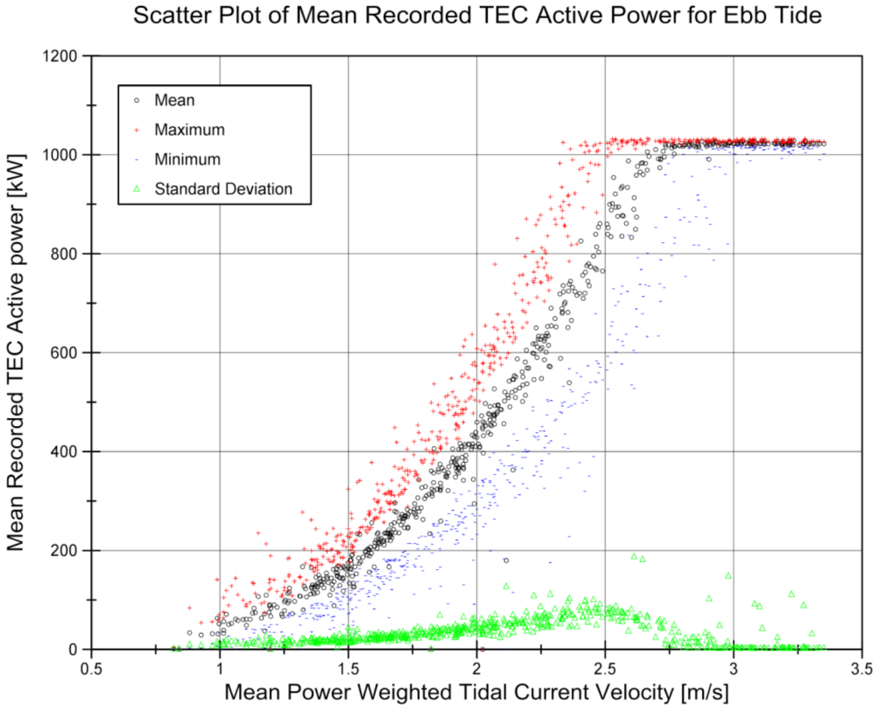

Figure 9-5: Active recorded power for ebb tide

10 PRESENTATION OF PREDICTED DATA

In addition to physical measurements (previous section) a predicted power curve is created using Garrad Hassan's Tidal Bladed software (version 4.4). The key inputs to the model that influence the power curve of the turbine are listed below.

1. Hydrofoil datasets – Stating the hydrofoils Lift, Drag and Moment coefficients. These are created using RFOIL.
2. Electrical and Mechanical Losses – Including bearing friction, gearbox, generator, transformer, frequency converter, auxiliary system (lubrication, cooling, instrumentation etc.). These are shown in Table 10-1 and Table 10-2.
3. Control system parameters – In particular optimal mode gain which governs the generator torque demand for a given generator speed. A value of 0.8 $Nm/(rad/s)^2$ is used for the optimal mode gain.

The predicted power curve is calculated by means of a steady simulation and hence neglects transient flow features such as turbulence, waves and velocity shear.

LSS Input Torque (kNm)	0	173	518	691	864	1100
Loss (kNm)	14	16.1	24.6	33.6	57.4	80

Table 10-1: Mechanical losses applied to predicted power curve in Tidal Bladed

Input Power (kW)	0	100	200	300	400	500	600	700	800	900	1000	1100	1200
Loss (kW)	24	36.786	43.923	49.689	54.997	60.064	64.979	69.785	74.508	79.165	83.768	88.324	92.840

Table 10-2: Electrical losses applied to predicted power curve in Tidal Bladed

11 PRESENTATION OF THE POWER CURVE

The measured data samples shown in the previous section are averaged into velocity bins of size 0.05 m/s and presented in Figure 11-1 with tabulated values in Table 14-1. Note that the IEC Guidelines (IEC, 2013), Section 8.7, specify the velocity range should be 50% of cut-in velocity (i.e. 0.5 m/s) to 120% of rated velocity (i.e. 3.24 m/s). In addition each velocity bin should have a minimum of 30 minutes of data and the complete data set 180 hours.

The (centre of bin) velocities presented are in the range 0.925 to 3.025 m/s for flood and 0.825 to 3.375 m/s for ebb. However, respecting the minimum of 30 minutes of sampled data per velocity bin (see Table 14-1) these ranges become 0.925 – 3.025 and 0.975 – 3.325 m/s for flood and ebb respectively. Hence the minimum velocity range is not met; however, this could be due to the stringent removal of samples with minimum power below zero (i.e. to remove shutdown events). It is also worth noting that the cases below cut-in velocity where power is observed are likely to be recorded at the end of a tide when the flow is decelerating from a higher value.

The total length of sampled data is 192 hours which respects the 180 hour minimum imposed in the standards.

Both flood and ebb power curves are similar which is encouraging to show the TEC performance in flow conditions that are quite different in terms of turbulence and shear profile (Smith, 2014).

The measured power curve is shown against two sets of predictions obtained using Tidal Bladed; steady and dynamic values. The dynamic predictions are obtained from a series of fatigue calculations; these being the cases used in the certification of DEEP-Gen IV (Newton, 2012) but with the RFOIL polars described in Section 10. Due to multiple calculations being performed at each flow speed (for different wave states) the results have been weighted and averaged according to the wave-scatter diagram used in the certification document.

Below rated velocity the measured values are higher than the theoretical value. The theoretical and measured predictions of rated velocity are very close and above rated the measured values are higher than the predicted values. The steady predicted performance curve is generated by neglecting unsteady effects such as velocity shear, turbulence and waves; these cause the large scatter observed in Figure 9-4 and Figure 9-5. These transient effects are taken into account for the dynamic values, which are much closer to the measured values. However, the individual effect of each of these on the performance is difficult to quantify and is one of the aims of the ongoing ReDAPT project. Other contributable transient effects, not the immediate focus of ReDAPT, include large scale flow meandering and depth varying directionality in the velocity profile.

Further differences between the measured and predicted curves can come from bathymetric and blockage effects. Theoretical work, for example (Garrett & Cummins, 2007; Whelan, Graham, & Peiró, 2009; Nishino & Willden, 2012), show the localised blockage can have a significant effect on the power coefficient. The channel occupied by the TEC is approximately 2km across from Eday to Muckle Green Holm which leads to an approximate channel blockage ratio less than 1%. This would not be considered significant enough to increase performance to the level that is seen in Figure 11-1. However, the blockage over the depth (approximately 40%) is large and could have a significant effect on the power. Tidal Bladed includes some options for including the effects of blockage. However, these are not documented and are not yet included in the present modelling strategy used here.

The measured and both predicted power curves also include a series of uncertainties; these are quantified in Section 12.

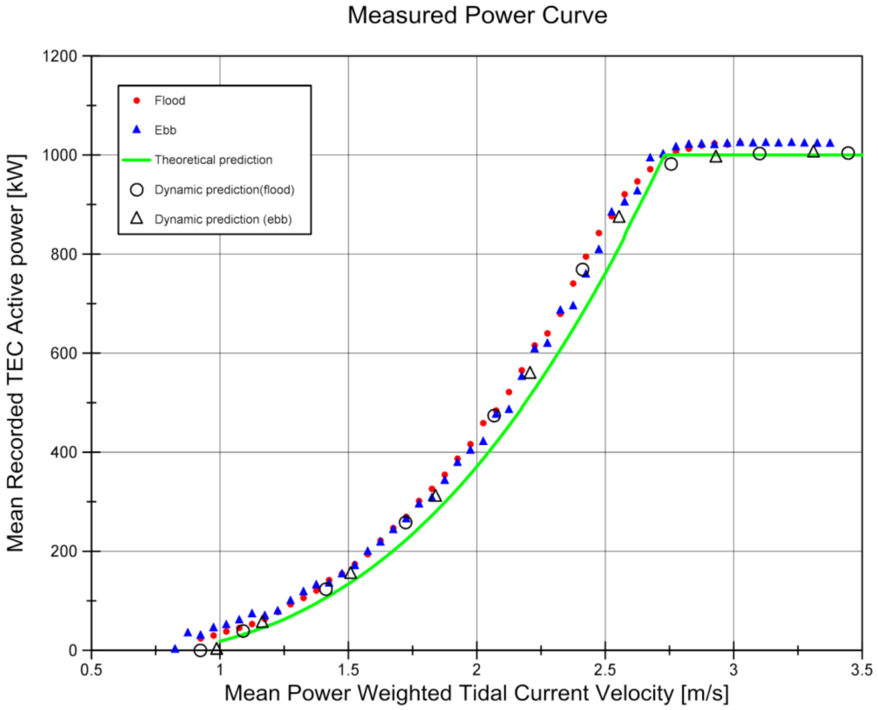

Figure 11-1: Measured power curve shown against theoretical and dynamic predictions

11.1 TEC Efficiency

The whole TEC system efficiency is defined by:

$$\eta = \frac{P}{\frac{1}{2}\rho A\, U^3}.$$

Where P = Turbine Power [W], ρ = Sea Water Density [1027 kgm^{-3}], A = Rotor Area [257 m^2], U = Flow Velocity [ms^{-1}]. This is shown in Figure 11-2, both tides show very similar results above rated velocity whereas below rated the ebb tide shows more spread in the results. The maximum efficiency for flood tide is 0.424 and for ebb 0.418. TEC efficiency should not be confused with the rotor power coefficient which is a measure of the rotor's hydrodynamic efficiency. This TEC efficiency includes all the mechanical and electrical losses in the whole system and so the rotor power coefficient is always larger than TEC efficiency.

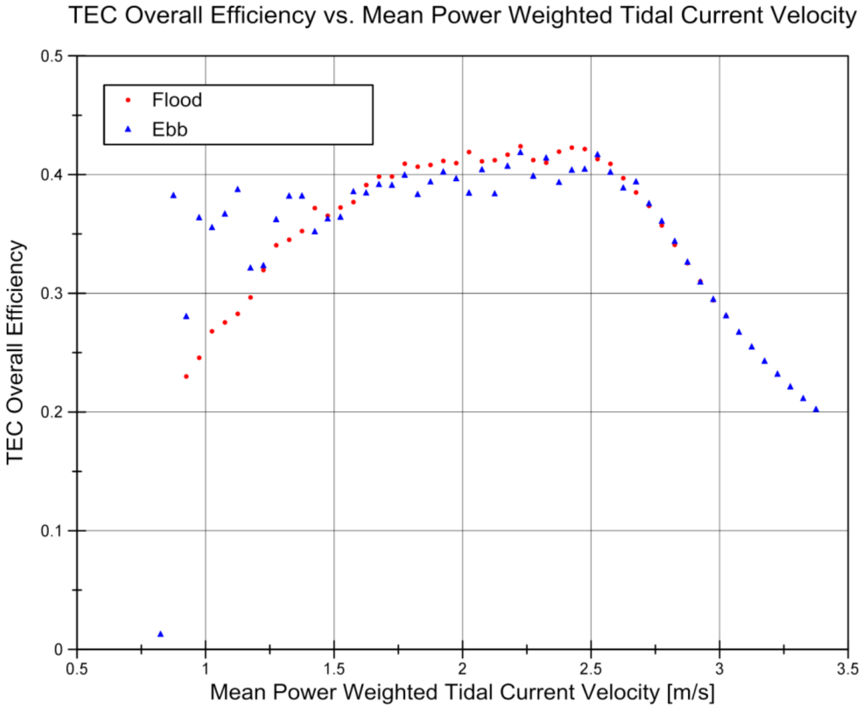

Figure 11-2: Overall efficiency of the TEC for flood and ebb tides

11.2 Turbine power estimation

The power curve presented in Figure 11-1 is created from measured shore power and thus includes losses due to the subsea cable and shore side transformer. These can be quantified using the following equation from a technical note (Palethorpe, 2013):

$$P_{loss} = \underbrace{3I_{6.6}^2 R_{cable}}_{\text{Cable losses}} + \underbrace{[3I_{6.6}^2 R_{LVTx} + 3I_{11}^2 R_{HVTx}]}_{\text{Transformer on-load losses}} + \underbrace{P_{Tx,no-load}}_{\substack{\text{Transformer} \\ \text{no-load losses}}}$$

By taking equivalent circuit completely referred to the 1 kV winding the R_{LVTx} term is 0.

The difference between assumed power at the TEC using the above losses and the measured power at shore is shown in Figure 11-3. Near the cut-in velocity the difference is greatest, approximately 5%, and reduces as velocity increases. In the regime from 1.5m/s up to rated velocity the losses are at their minimum (less than 2%) before levelling off at approximately 3% above rated.

Term	Value	Reference
R_{cable}	3.6 x 0.154 ohm = 0.5544 ohm	EMEC cable spec 20degC DC resistance value
I_{11}	$= \frac{P_{real11kV}}{\sqrt{3}\,V_{11kV}}$	Measured values
$I_{6.6}$	$= I_{11}\left(\frac{11}{6}\right)$	Calculation
R_{HVTx}	1.18 ohm	From Tx full load losses of 15237W from Merlin Gremlin
$P_{Tx,no-load}$	1593 W	Tx data sheet
V_{11kV}	11000 W	Assumed constant
$P_{real11kV}$		Measured shore power

Table 11-1: Values of losses from turbine to shore power

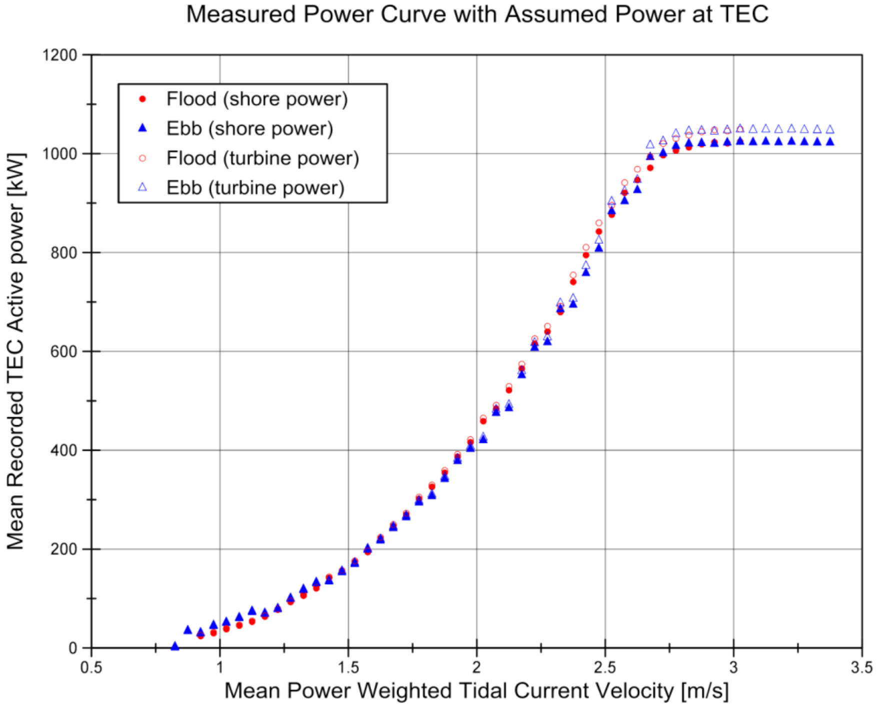

Figure 11-3: Power at turbine calculated from shore power and assumed losses

12 UNCERTAINTIES

12.1 Measured Performance Curve

12.1.1 Velocity bins

Some uncertainty is associated to the choice of ADCP bins, and their weighting. Due to the change in bathymetry and depth between ADCPs and TEC the choice of hub-height reference is made complex. This is further complicated by the TEC centre line not being perfectly horizontal, and hence changes during a yaw operation. The method used for the measured power curve is described in Section 9.2 and by Figure 9-2. The hub-height reference depth is deduced from pressure transducer on the TEC, this is then correlated to an equivalent ADCP bin measured from the surface. The described approach is deemed suitable and of reasonable accuracy, however, it is possible there is an offset error which has been quantified as a maximum of 2m. The effect of an incorrect reference bin by plus and minus 2m is shown in

Figure 12-1 and Figure 12-2, with results showing sensitivity to the measured rated velocity by approximately 0.05 m/s per 2m offset to the reference depth. This represents an uncertainty of 2% to the measured rated-in velocity.

12.1.2 ADCP Positions

The positions of both ADCPs are described in Table 5-3 and Figure 5-3. ADCP SE is approximately 1.1D from the line of principal ebb direction. This is twice the distance recommended by the IEC standards. To properly assess the level of uncertainty that can be associated with this requires some knowledge on the spatial change in velocities in the test area.

12.1.3 Data synchronisation

Time synchronisation between ADCP NW, ADCP SE and TEC controller datasets may be off due to being recorded on different clocks. Instantaneous data was compared and matched well and so any inaccuracies are assumed small and less important due to the time bin size of 10 minutes.

The upstream flow is measured before the same volume of water meets the turbine. This lag is inversely proportional to the flow speed and long length-scale turbulence may skew the flow measurements. Accounting for this will add much complexity to the analysis, although a simpler offset could be applied based on the distance between TEC and the mean flow speed.

12.1.4 Data quality

The ADCP data has not yet been fully quality controlled (QC) although it is considered sufficient quality for 10 minute average values.

12.1.5 Turbine heading

Yaw heading of the turbine relative to the flow was aligned using historic data rather than measured due to instrument failure on the turbine. The exact flow direction was not considered for the presented power curves, the flow velocity was the flow magnitude, rather than the flow vector directly in line with the turbine heading. This is in agreement with the IEC standards.

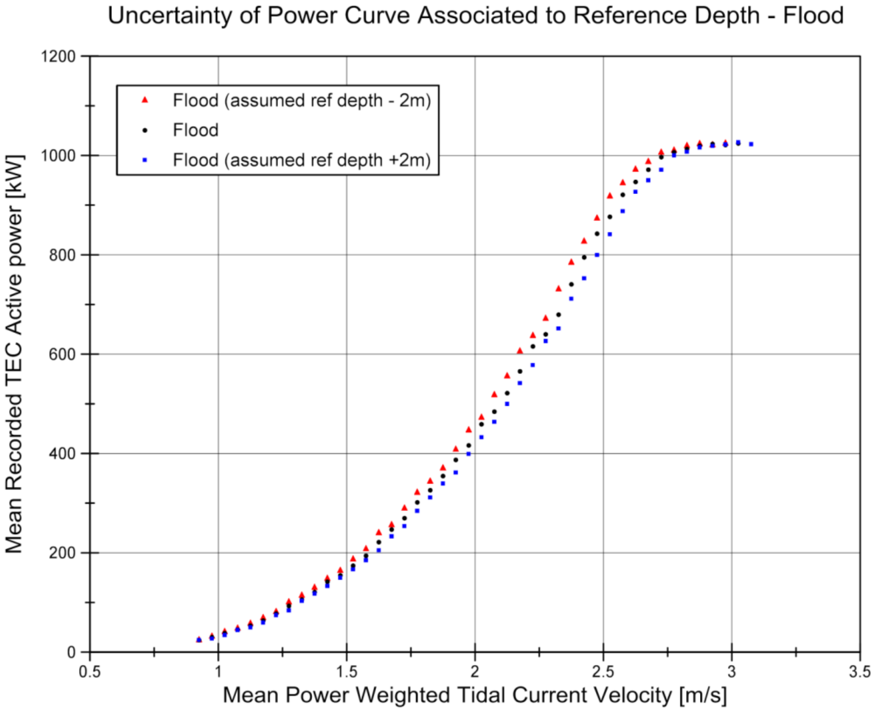

Figure 12-1: Power curve uncertainty associated to reference depth for flood tide

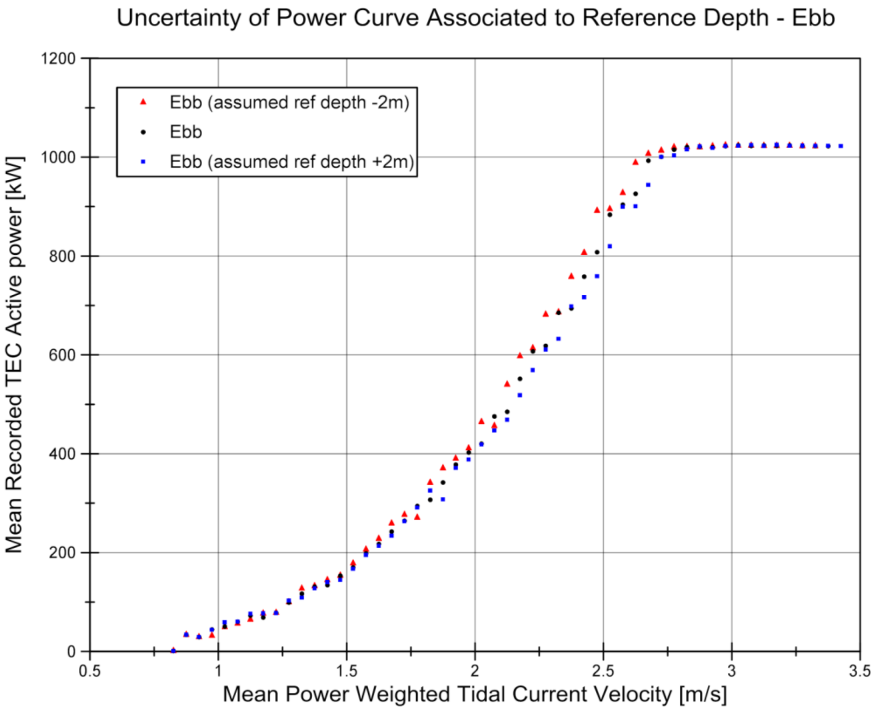

Figure 12-2: Power curve uncertainty associated to reference depth for ebb tide

12.2 Uncertainties in Predicted Performance Curve

The predicted performance curve has several sources of potential errors which can arise from the inputs described in Section 10.

12.2.1 Blade section polars

The hydrodynamic coefficients associated to each of the blade sections are vital to the values in the predicted rotor power coefficient. RFOIL was used to create these polars for the predicted steady and dynamic power curves. RFOIL is a derivative of X-FOIL (Drela), a tool for analysis of isolated aerofoils. RFOIL has improved boundary layer description and can take into account effects of rotation. However, both X-foil and RFOIL have been shown to under predict the drag coefficient by approximately 10% when compared to experimental data, see (van Rooij, 1996) and (Grasso, 2010) for example.

12.2.2 Losses

Losses are included in the predicted power curve by means of mechanical and electrical losses; see Table 10-1 and Table 10-2. These were originally derived and scaled from DEEP-Gen III; the 500kW predecessor to the TEC that is the focus of this document. Sensitivity to these losses are not easy to quantify as they are one of the primary assumptions before building up the Tidal Bladed model, and subsequent modelling decisions are based on these. An increase in mechanical losses would lead to an increase in rated velocity. Increased electrical losses would require higher demanded generator torque to achieve the same rated power, again with an increased rated velocity. It appears that the losses in the model are too high, since the real power output above rated flow speed is greater than 1MW whereas the model is exactly 1MW.

12.2.3 Control system

This is most sensitive in the section of the curve before rated velocity, as rated power is observed above this value. The optimal mode gain governs the targeted optimal tip-speed ratio below rated velocity and such adjusting the value has a significant effect on this although not necessarily on the observed electrical power.

12.2.4 Model validation

In addition to the uncertainties listed above there are some associated to the modelling approach in Tidal Bladed, which is essentially a black-box, i.e. the numerical method is hidden from the user. Tidal Bladed uses blade-element momentum theory (BEMT) to produce the predicted performance curve; this is a well validated method in both Tidal Bladed and other models for experimental TECs, see (Bahaj, Batten, & McCann, 2007) for example. Full validation is one of the focus points of the ongoing ReDAPT project.

12.2.5 Transient effects

Including transient effects lead to a much closer match between the measured values and those obtained with Tidal Bladed. However, the individual influence of the transient effects is not quantified and it is possible there is a cancellation of errors to obtain these improved predictions. As already discussed, understanding these transient effects and validation of them within Tidal Bladed is ongoing within the ReDAPT project.

13 CONCLUSIONS

This document presents a measured power curve for DEEP-Gen IV using data obtained during October and November 2013 at EMEC. The document has been produced to meet the standards of IEC 62600-200 (IEC, 2013). Generally the standards have been met, although there are several areas where they were not achieved:

1. Position of ADCP SE. This was used to characterise the velocity in the flood direction. The ADCP was approximately 1.1D off the line of principal flow direction through the TEC. This has been used to advise a new location for placement of the ADCPs for future deployments.
2. Data availability. Including slack tides the data availability was 72%. Further operating data over a period with less machine testing in order to achieve the 80% specified minimum.
3. Velocity range. The presented power curve did not give values for velocities at 50% of the cut-in velocity. This was likely due to stringent selection criteria in the curve creation as well as a lack of available data.

The measured power curve has been presented against predicted steady and dynamics power curves obtained using Tidal Bladed. The measured power curve is higher than the steady curve although both show similar shape and give close values of rated velocity. Inclusion of transient effects in the dynamic curve give closer agreement to the measured values.

Several differences between measured and predicted power curves are identified. Understanding the influence of the individual transient effects is important for better interpretation of the predicted results.

Areas of uncertainty are identified in both measured and predicted power curves. For the measured values the most uncertainty comes from the correct velocity bins to use in the mean power weighted velocity, and the spatial variation of velocity across the site. For the predicted curve modelling uncertainty is the biggest issue, including the hydrofoil polars and validation of the Tidal Bladed model.

The power curve document meets the majority of the standards of IEC 62600-200 (IEC, 2013) and is thus deemed an acceptable document. A revised power curve should be produced following future deployments of DEEP-Gen IV to better meet the IEC criteria. The areas of uncertainty and difference for and between both measured and predicted power curves are areas of ongoing interest as part of the ReDAPT project and will be better quantified as this research and understanding progresses.

14 POWER CURVE DATA

Velocity range [m/s]		Flood		Ebb	
Minimum	Maximum	Mean Power [kW]	No. data points (10 min sample)	Mean Power [kW]	No. data points (10 min sample)
0.800	0.849			0.91	2
0.850	0.899			33.73	1
0.900	0.949	23.99	4	29.22	1
0.950	0.999	30.02	4	44.39	4
1.000	1.049	38.04	9	50.39	6
1.050	1.099	45.11	10	59.99	3
1.100	1.149	53.07	25	72.62	7
1.150	1.199	63.40	15	68.60	10
1.200	1.249	77.44	21	78.22	4
1.250	1.299	93.04	19	98.84	10
1.300	1.349	105.83	20	116.98	7
1.350	1.399	120.76	17	130.75	18
1.400	1.449	141.81	21	134.06	14
1.450	1.499	154.53	23	153.28	19
1.500	1.549	174.07	21	170.03	19
1.550	1.599	194.07	22	198.37	12
1.600	1.649	221.29	18	217.26	20
1.650	1.699	246.74	16	242.32	21
1.700	1.749	269.59	26	264.32	16
1.750	1.799	301.64	17	294.23	14
1.800	1.849	325.79	22	306.78	15
1.850	1.899	354.63	21	341.85	15
1.900	1.949	386.89	15	377.83	24
1.950	1.999	416.03	20	402.33	16
2.000	2.049	458.69	19	420.32	17
2.050	2.099	484.21	18	475.45	20
2.100	2.149	521.26	12	484.93	15
2.150	2.199	565.35	11	551.67	12
2.200	2.249	615.45	15	607.12	13
2.250	2.299	639.90	13	618.18	16
2.300	2.349	679.29	12	685.17	11
2.350	2.399	740.50	14	693.99	11
2.400	2.449	794.68	16	758.28	10
2.450	2.499	842.42	6	807.67	9
2.500	2.549	876.52	11	883.60	11
2.550	2.599	920.69	8	903.76	9
2.600	2.649	946.63	10	925.96	11
2.650	2.699	971.34	14	992.87	5
2.700	2.749	996.58	10	1000.74	9
2.750	2.799	1006.14	6	1015.04	7
2.800	2.849	1012.74	5	1020.28	8
2.850	2.899	1019.27	9	1020.93	10
2.900	2.949	1022.87	5	1019.57	10
2.950	2.999	1020.85	1	1022.18	9
3.000	3.049	1024.34	2	1023.95	10
3.050	3.099			1022.84	11
3.100	3.149			1023.73	7
3.150	3.199			1022.81	11
3.200	3.249			1023.70	8
3.250	3.299			1022.76	8
3.300	3.349			1022.58	4
3.350	3.399			1022.13	1

Table 14-1: Power curve data